DEPTH PROBING SOFT X-RAY MICROPROBE (DPSXRM) FOR HIGH RESOLUTION PROBING OF EARTH'S MICROSTRUCTURAL SAMPLES

Patrick N. Dikedi, Adedeji A. Adetoyinbo
Veritas University Abuja FCT, University of Ibadan, Oyo State

Abstract

The Cambrian explosion; occurrence of landslides in very dry weather conditions; rockslides; dead, shriveled-up and crumbled leaves possessing fossil records with the semblance of well preserved, flat leaves; abundance of trilobite tracks in lower and higher rock layers; and sailing stones are enigmas demanding demystifications. These enigmas could be elucidated when data on soil structure, texture and strength are provided by some device with submicrometre accuracy; for these and other reasons, the design of a Depth Probing Soft X-ray Microprobe (DPSXRM), constituting a rotating X-ray window is being proposed; it is expected to deliver soft X-rays, at spatial resolution, $\varsigma \geq 600nm$ and to probe at the depth of 0.5m in 17s. Assessing subsurface stratigraphy is possible with the DPSXRM.

The microprobe is portable compared to a synchrotron radiation facility (Diamond Light Source has land size of $43,300m^2$); spatial resolution, $\varsigma \geq 600nm$, of the DPSXRM surpasses those of the X-ray Fluorescence microanalysis(10μm), electron microprobe (1-3μm), and ion microprobe (5->30μm); the DPSXRM has allowance for multiple targets.

Amongst other major optical components, a Fresnel Zone Plate (FZP) and Rotating X-ray Window are incorporated into the design to ensure that the desired image resolution is achievable and that the X-ray window membrane material survives the heat flux impartation on it.

Reflecting, refracting, diffracting and (or) absorbing optics are identified as techniques needed to achieve this resolution. Vanadium and Manganese membranes are proposed owing to respective 4.952KeV $VK\alpha_1$ and 5.899KeV $MnK\alpha_1$ X-rays emitted, which best suits micro-probing of Earth's microstructural samples.

Compound systems like the Kirk-Patrick and Baez, electromagnetic lenses, small apertures and Abbe sine condition are considered to reduce or remove astigmatism and coma and spherical aberrations—leading to good image quality.

Results are presented alongside, and relevant graphs are plotted. Magnification values of $-1.5 \leq M \leq 1.5$, at $-70^0 \leq \theta' \leq 75^0$ when $-30^0 \leq \theta \leq 30^0$ satisfied Abbe Sine Condition.

The nth zone radius increases with the distance of separation of the DPSXRM's electron gun and the zone plate. 5.899KeV $MnK\alpha_1$ and 4.952KeV $VK\alpha_1$ soft X-rays will travel a distance of 2.75mm to form circular patches of radii 2.2mm and 2.95mm respectively. Zone plate with nth zone radius of 1.5mm must be positioned 1.5mm and 2mm from the electron gun if circular patches must be formed from 4.952KeV $VK\alpha_1$ and 5.899KeV $MnK\alpha_1$ soft X-rays respectively.

The focal lengths of $0.25\mu m \leq F \leq 1.50\mu m$ and $0.04\mu m \leq F \leq 0.2\mu m$ covered by 4.952KeV $VK\alpha_1$ and 5.899KeV Mn $K\alpha_1$ soft X-Rays, will occupy circular patch of area $0.03mm^2 \leq A \leq 0.2mm^2$ respectively.

The spatial resolution of $244nm \leq \varsigma \leq 1460nm$ is attainable for focal lengths of $38.1nm \leq F \leq 229nm$ and $32.0nm \leq F \leq 1460192nm$ covered by 5.899KeV Mn $K\alpha_1$ and 4.952KeV $VK\alpha_1$ soft X-rays, respectively.

Simulation results from COMSOL Multiphysics software uncover some deformations in Vanadium and Manganese microstructures.

Keywords: *Cambrian explosion, Soft X-Rays, Microprobe, Astigmatism, Coma*

Introduction

The Earth is a custodian of samples which conceals a lot of useful information awaiting to be unraveled when they are micro-probed by high resolution techniques and devices; microstructure of earth samples under microprobes, will reflect the entire geologic and stress history of earth deposits. Depositional history, weathering history both (physical and chemical) and environment of the deposit are all concealed information impregnated in the Earth's microstructures—these information could be uncovered by some soft-x ray releasing high resolution microprobe device; soft x-rays have been identified (Pfauntsch, 2001) to occupy a wavelength of $\lambda \approx 100eV$ *to* $5\ KeV$ $(10nm$ *to* $0.1\ nm)$ on the electromagnetic spectrum.

It is salient noting that microstrucutres could turn out flocculated; and these lumpy structures result during sedimentation in all depositional environments such as marine, brackish or in freshwater (Holtz and Kovacs, 2010).

Cambrian explosion, the sudden appearance of major animal groups at the bottom of the fossil

record, the occurrence of landslides in very dry weather conditions; dead, shriveled-up and crumbled leaves possessing fossil records with the semblance of well preserved, flat leaves, abundance of trilobite tracks in lower and higher rock layers and sailing stones occurrences are enigmas demanding demystifications. These enigmas could be elucidated when data on soil structure, texture and strength are provided by some device with submicrometre accuracy; for these and other reasons, the design of a Depth Probing Soft X-ray Microprobe (DPSXRM), constituting a rotating X-ray window is being proposed; it is expected to deliver soft X-rays, at spatial resolution, $\varsigma \geq 244$nm and to probe at the depth of 10m in 5mins. 40s. Assessing subsurface stratigraphy is possible with the DPSXRM.

The DPSXRM offer promises such as Imaging of internal compositional—microstructures; microstructures could reveal micro-faults, micro-textural and fabric information. Additionally, It measures soil strength in Kilopascal (KPa).

Literature Review

Blair and Hedges,(2004), Sanderson *et al* (2004), Jones III *et al* (2009), Erwin *et al* (2011), Shu *et al* (2002), Dupraz *et al* (1995), Morris (2000) and Eizirik *et al* (2001) , Park *et al* (2013) have made fragmentary contributions on Impact-induced seismic activity on Asteroid, laser ablation for deflecting asteroids, sliding rocks, trilobites and testing the Cambrian explosion.

It has become necessary for regions dotted with these catastrophic events to be micro-probed by some device with high spatial resolution for the purpose of demystification. Though high precision devices have pre-existed (Minh *et al* 2002), this research is delved towards the design of the DPSXRM, which shows promises of outperformance.

DPSXRM is a table-top device which will be made of the electron gun; the gun is made of a tungsten filament (electron source) positioned in a ceramic holder which releases electron at electron energy of ≤ 15 KeV and at electron current of ≤ 0.5 mA. Characteristic K_α X-rays will be produced when fast moving electrons (beams) emitted from the electron gun impinges on the membrane of a rotating X-ray window; the choice of membrane material ismade by simulations using COMSOL Multiphysics Software, alongside relevant excel programs. However, Vanadium and manganese are being ticked as potential target materials because of the promises they hold in terms of their thermal and optical properties best suited for soft X-ray generation.

Numerous membrane materials have been discovered (Haschke, 2014; Dikedi, 2012), for the purpose of micro-probing owing to their characteristic K_α X-rays.

Carbon, Aluminum, Titanium and Chromium targets releases 0.278KeV C K_α X-rays, 1.49KeV Al K_α X-rays, 4.5KeV Ti K_α X-rays and 5.4KeV Cr K_α X-rays respectively. These X-Rays take their exit from a 100nm silicon nitride membrane. There is the vacuum chamber housing the X-Ray window; the chamber is made of an inlet and an outlet for inflow and outflow of Helium gas (He); mounted on the chamber are regulators to regulate the pressure within the X-Ray chamber; regulation is necessary to prevent X-Ray window membrane from breaking. Existing microprobes are unable to accommodate more than one target materials. The silicon nitride frame of DPSXRM is built with enough room to accommodate a range of targets or membrane materials and to allow for flexibility in its operation (Folkard , 2005; Pfauntsch, 2001); changing target materials imply that X-Ray photon energy will change leading to change in power (to produce this photon energy) and change in the focal length of the X-Ray lenses. The window is also fitted with an electric motor to initiate rotation.

The use of impinging electrons and X-Rays in probing material structures are well noted, however the use of polarized soft X-Rays for nanomagnetism (Laan *et al*., 2014) at the Diamond Light Source Synchrotron facility is no more than a mere proposal; inferentially, soft X-ray-related researches are very virgin areas awaiting to be explored.

X-ray absorption spectroscopy is being identified by Bunker, (2011) and corroborated by Michette (2011), as a powerful tool in the elucidation of material structure and environment.

Cyclotrons for Positron Emission Tomography (PET) radioisotope production are employed for radio biological and radiophysiological studies.

Transmission Electron Microscopy (TEM) is a well-established and powerful technique (Sourty *et al*, 2008) to explore matter down to the atomic scale but information derived from this technique is limited to two dimensions—there is the need for volume information since real world objects have a three dimensional character.

It is well established (Sanloup *et al*, 2013) that X-Rays have been made to probe molten magma at conditions of the deep Earth mantle; results show that early in the history of the Earth, when it started crystallizing, magmas may have been negatively buoyant at the bottom of both, the upper and lower mantle, resulting in the existence of two magma oceans, separated by a crystalline layer.

Ion-Exchange-Resin Membrane Technique (IERMT) has been adopted (Liangyuan *et al*, 1983) to determine the relative concentration of Rare-Earth Elements (REE) by X-Ray Fluorescence (XRF) with controlled area density kept at $0.0003 gcm^{-3}$.

It is well reported in 2013 by German Research Centre for Geosciences, that high energy X-rays, produced by X-ray Raman Scattering (XRS), an inelastic X-ray scattering process, may be made to pass through a diamond anvil cell (a high pressure apparatus), reaching the sample located in the cell. Analyzed parameters for trace elements in deep well, well, borehole and stream water are well documented (Adetoyinbo, Bello and Hammed, 2013); X-Ray Fluorescence spectrometer is reputable (Wirth and Barth , 2013) for bulk chemical analyses of large fractions of geological materials such as trace elements in rocks—it cannot make analysis at small spot sizes such as 2-5μm. The DPSXRM is well able to cover the imaging of this particle size since it is well able to image microstructures down to 244nm size.

Materials and method

Schematics and descriptions

Schematics and introductory descriptions of some parts of the microprobe are considered:

Penetrometers

The inclusion of penetrometers will ensure provision of very accurate information on soil strength or resistance to penetration to some depth; it is worth noting that measurements of soil strength in KPa, are affected by moisture, porosity and rock content. It is well established that (Kees , 2005), when combined with other information, such as soil moisture, structure, and texture, data from penetrometers can contribute to a more accurate picture of soil properties; penetrometers encourage in situ measurements. The test involves pushing cone penetrometers steadily into the ground; while soil strengths or soil penetration resistance, encountered at various depths are measured. For accurate readings, the insertion must be done at 30mm/s-the handheld type can probe 0.5m deep into the subsurface in 17s

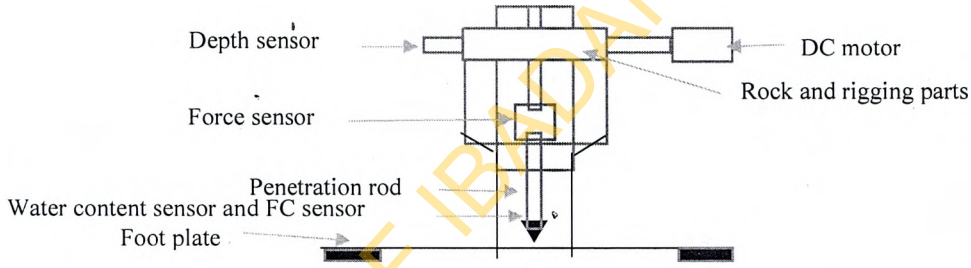

Figure 1 A schematic of a penetrometer resting on a foot plate.

Fresnel Zone Plate

At short wavelengths particularly in the soft X-ray region, the use of zone plates is employed because of their ability to form images at very high spatial resolution (Chao *et al*.,2006).

Fresnel zone plate lens is one of the focusing devices used in synchrotrons. Zone plates form a focus by using constructive interference of rays from adjacent zones.

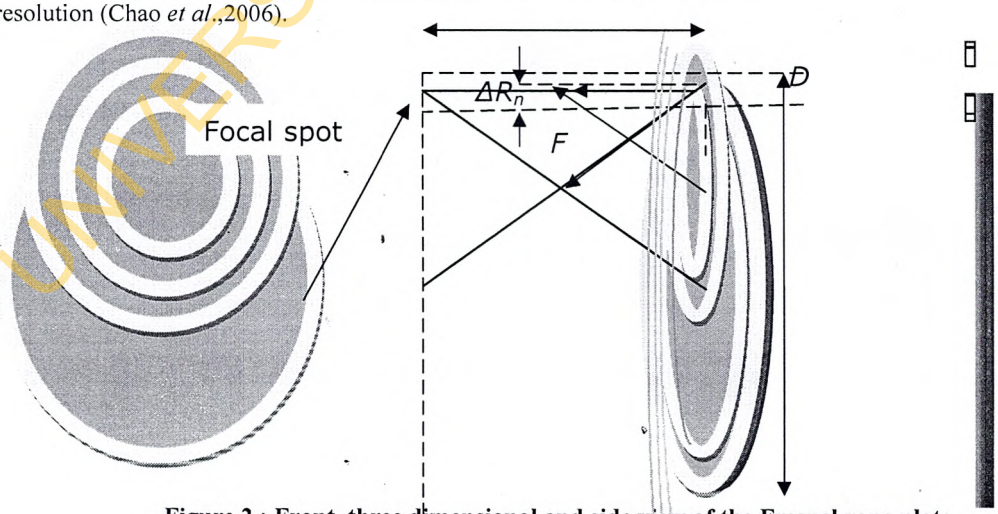

Figure 2 : Front, three dimensional and side view of the Fresnel zone plate

Interactions of impinging electrons with Vanadium membrane materials .

Within the microprobe, electrons will be emitted when the filament in an electron gun is heated. These electrons will then be released as a beam by accelerating them down a column at very high voltages; existing voltage ranges had been 15 000 to 20 000v.

Very saliently, it must be noted that electrons will further be made to pass through lenses that will (1) condense the beam (2) remove aberrations (3) focus the beam.

Thereafter, focused electron beam will be made to impinge on a vanadium or manganese material (membrane) overlying a rotating window; this window will be encased in an X-ray vacuum chamber within a pressure regulated environment—usually at 0.01mbar.

Upon impingement, electrons will interact with the atoms within the membrane; this interaction means that electrons are scattered by membrane atoms into an interaction volume; this interaction will thereafter lead to production of characteristic Soft X-rays; characteristic X-rays with characteristic energies depend on the type of membrane material impinged upon.

It is salient noting that characteristic Soft X-rays, emitted from membranes like those from vanadium are generated within the aforementioned interaction volume; the size of this volume may be determined by the density of the membrane and energy of the impinging electron beam. It is well established that electron beam of 15 000v infers that a 2μm diameter interaction volume does exist

Emitted Soft X-rays are then directed to a Fresnel Zone plate (FZP); apertures are employed to block unwanted X-rays. Selected focused X-rays are made to pass through the FZP, to an earth sample or biological specimen, placed in a special holder for micro-probing; the UV assay microscope is positioned directly above the sample for investigation.

Relevant equations for this investigation are enlisted hereunder:

$$\delta E(KeV) = 88.5\frac{E^4(GeV)}{R(m)} \quad (1)$$

$$\lambda_c(nm) = 0.559\frac{R(m)}{E^3(GeV)} = \frac{1.864}{B(T)E^2(GeV)} \quad (2)$$

where B is the magnetic field. The characteristic wavelength, or the corresponding characteristic energy,

$$\varepsilon_c(KeV) = 2.218\frac{E^3(GeV)}{R(m)} \quad (3)$$

The emission angle, θ, of radiation varies with photon energy but may be approximated to:

$$\theta \sim \frac{m_e c^2}{E} \quad (4)$$

The implication of this expression is that the radiation is well collimated about the forward direction.

It is well established that (Michette, 2007) that high beam energies, small focused spot sizes, and short pulse lengths are needed as requirements for high irradiance.

$$\delta(\omega) = 1 - \left(1 - \frac{n_e e^2/m_e\varepsilon_0}{\omega^2}\right)^{\frac{1}{2}} \quad (5)$$

The transmission of lens, T depends on the X-Ray wavelength, λ, the lens material, the profile $x(y)$ and the distance of separation of individual lens centres, d; and may be expressed as:

$$T = \frac{1}{\pi R_0^2}\int_0^{R_0} 2\pi\gamma x exp\left[-\frac{4\pi\beta N}{\lambda}(x(y) + d)\right]dy \quad (6)$$

Fresnel Zone plate, which are circular diffraction grating made by electron-beam lithography, is incorporated into the design and the area of its nth zone may be expressed as:

$$\pi(r_n^2 - r_{n-1}^2) = \pi[n\lambda f_1 - (n-1)\lambda f_1] = \pi\lambda f_1 \quad (7)$$

The width of the nth zone, d_n is given by:

$$d_n = r_n - r_{n-1} = \sqrt{n\lambda f_1} - \sqrt{(n-1)\lambda f_1} = \sqrt{n\lambda f_1}\left[1 - \left(1 - \frac{1}{n}\right)^{\frac{1}{2}}\right] \approx \frac{r_n}{2n} \quad (8)$$

This equation leads to an expression for the first order focal length, f_1 given by:

$$f_1 = \frac{r_n^2}{n\lambda} = \frac{D_n}{\lambda} \quad (9)$$

$W\text{ere}, D_n$ is the diameter of the zone plate. Since D is the overall zone plate diameter and d is the outer zone width

$$f_1 = \frac{Dd}{\lambda} \quad , \quad (10)$$

The spatial resolution of the zone plate incorporated in the design, for an incoming wave is expressed according to the Raleigh criterion as

$$\varsigma = 1.22\, d \quad (11)$$

Where ς, is spatial resolution; if we set ς=0.45μm, then going by equation 10, the outermost zone width, d =0.368115μm; meaning that if ς≥0.45μm, then the outermost zone width, $d \geq 0.368115\mu m$. The value of spatial resolution, ς, is limited by X-ray photon energy of 4.952KeV (0.25nm) and 5.899KeV (0.21nm) for Vanadium and Manganese respectively.

$$\theta \sim \frac{m_e c^2}{E} \quad (12)$$

The emission angle for a 4.952KeV VKα_1 soft X-Rays is calculable from the expression above:

$$\theta_V \sim \frac{9.10938291X10^{-31}kgX8.9875518x10^{16}m^2s^{-2}}{7.93397835X10^{-16}\,J} = 103.190413634^0 \approx 103.2^0$$

Additionally, the emission angle for a 5.899KeV MnKα_1 soft X-Rays is calculable from the expression above:

$$\theta_{Mn} \sim \frac{9.10938291X10^{-31}kgX8.9875518X10^{16}m^2s^{-2}}{9.45123956\ X\ 10^{-16}J} = 86.6246699704^0 \approx 86.6^0$$

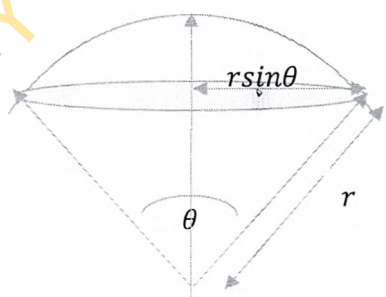

Figure 3: A schematic depicting the conic section of a beam of electrons released at an emission angle, θ.

Employing compound systems like the Kirk-Patrick and Baez, small apertures and obeying the Abbe sine condition, will ensure that astigmatism, coma and chromatic aberrations are reduced or eliminated—leading to good image quality.

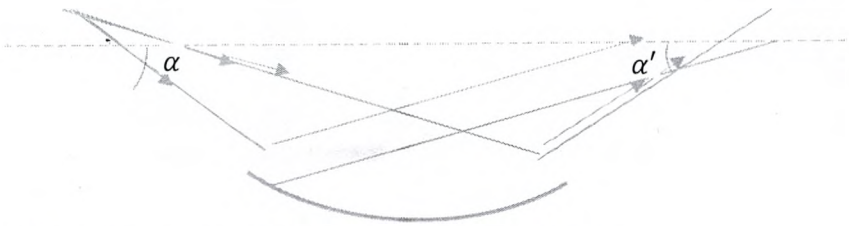

Figure 4: The set up helps to satisfy Abbe Sine condition

Reduction of coma is achievable, if Abbe sine condition is satisfied—all geometrical paths traceable through optical system(s) must give the same magnification:

$$M = \frac{sin\alpha}{sin\alpha'}$$

Where α, is the angle of ray coming from an object; α', is the angle of ray arriving at an image; M denotes magnification. The set up in figure 4obeys Abbe Sine condition; here, two reflections in two dimensions are needed. This set up eliminates coma

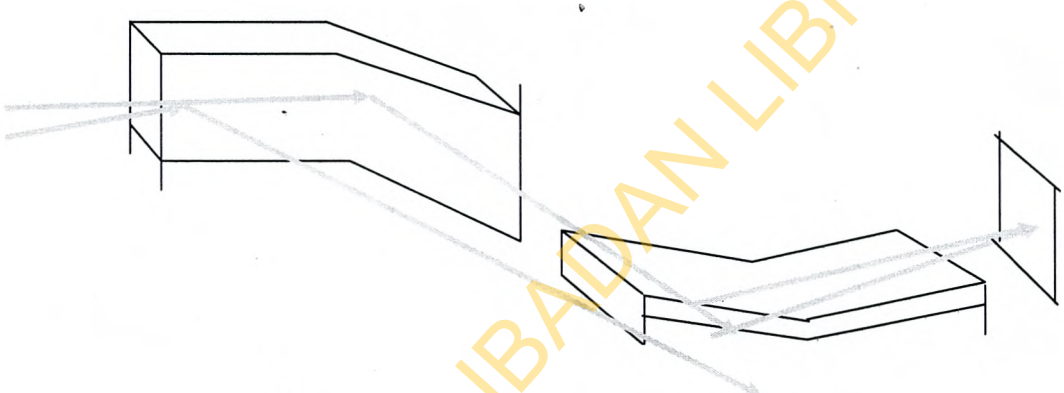

Fig. 5: Schematic of the Kirk-Baez Patrick (K-B) mirror configuration which provides vertical and horizontal focus.

Figure 5 is a schematic of Kirk-Baez Patrick (K-B) mirror configuration, which ensures a focus along the horizontal plane and yet another along the vertical plane; it is well established that this mirror system ensures high mechanical and thermal stability, and a short focal length which allows for a high source demagnification. The advantages of the K-B mirror system are its ability to deliver higher photon flux and its achromaticity (Barrett, 2011)

The KB mirror system (KB), a crossed mirror system, has been specially designed at the European Synchrotron Radiation Facility (ESRF). This mirror arrangement is based on elliptically shaped, fixed-focus Ni coated mirrors. It does achieve a spot size of 0.35 x 0.7μm^2 with a photon flux of 7.10^{10} photons/s; additionally, it provides both very high accuracy and flexibility. This mirror arrangement reduces or eliminates astigmatism.

Results

The result reveals that zone plateof focal length 50 and 45nm will focus 5.899KeV MnK$\alpha_1$and 4.952KeV VKα_1 soft X-rays to 244nm spot size. Figure 7 relates how the spot sizes for both 5.899KeV MnK$\alpha_1$and 4.952KeV VKα_1 soft X-rays improve with decreasing focal lengths.

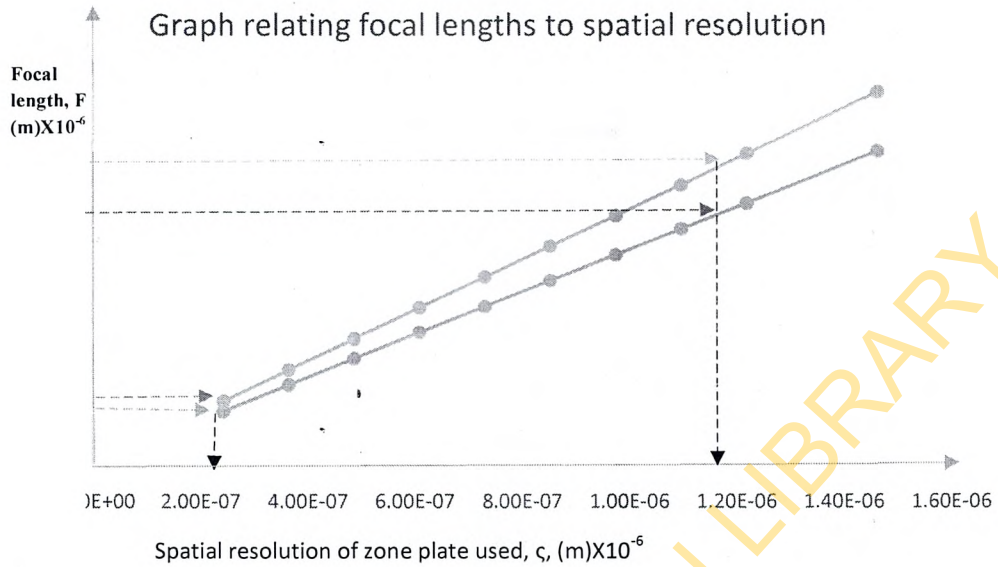

Figure 7: Graph relating focal lengths of zone plate to its spatial resolution

Furthermore, area of zone plate increases with its focal length. Manganese membrane shows greater focal length increase with zone plate area when compared to vanadium.

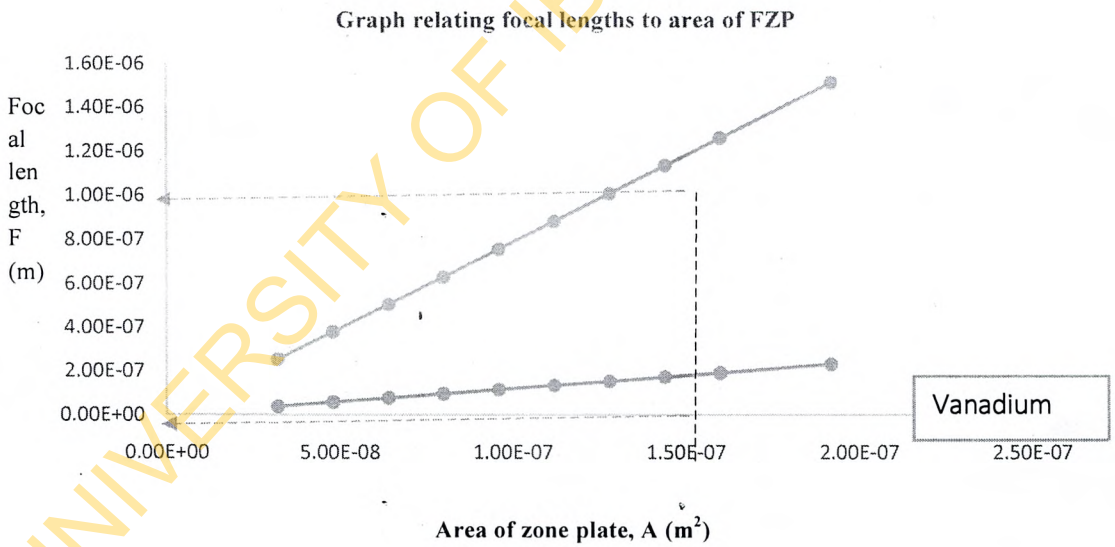

Figure 8: Graph relating focal lengths to area of FZP

Figure 8 reveals that the focal lengths of 0.18μm and 1.14μm are covered by 4.952KeV VKα_1 and 5.899KeV MnK$\alpha_1$soft X-rays emitted through zone plate disc of area 0.15μm^2. Clearly, result reveals that focal length elongates with increasing disc area of zone plate used.

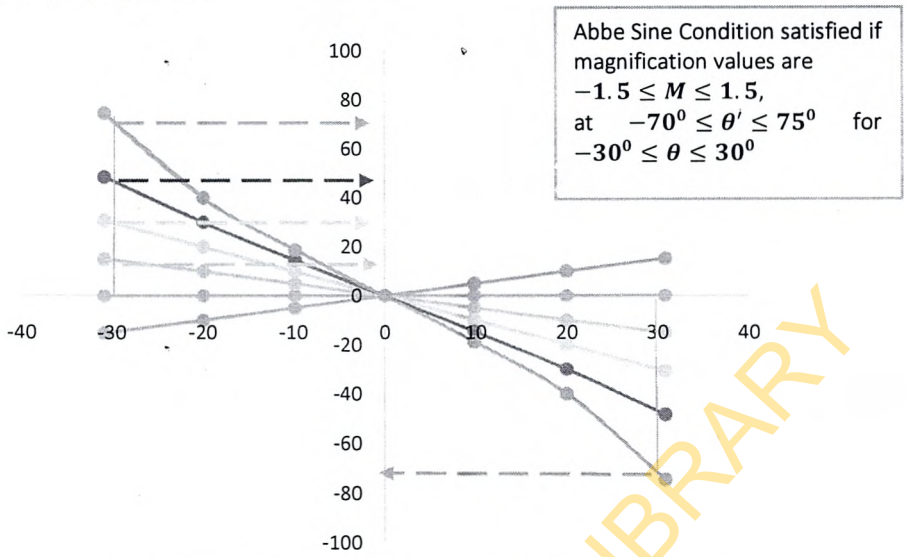

Figure 9: Graph indicating how Abbe Sine condition is satisfied with varying magnifications and the corresponding angle of ray departing from an object; and arriving at an image.

Clearly, Abbe Sine Condition is satisfied if magnification values are $-1.5 \leq M \leq 1.5$, at $-70^0 \leq \theta' \leq 75^0$ for $-30^0 \leq \theta \leq 30^0$.

Figure 10 (a) : Simulated structure of Vanadium displaying transient thermal stress distribution in time steps of 0.2, 0.4, 0.6, 0.8 and 1.0s

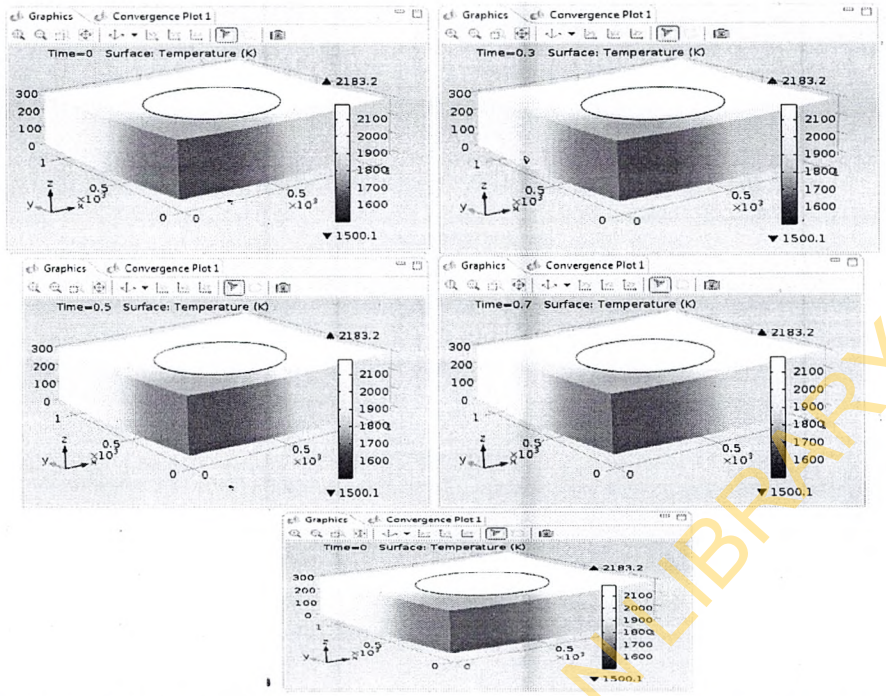

Figure 10 (b): Simulated structure of Vanadium displaying transient temperature distribution in time steps of 0, 0.3, 0.5, 0.7 and 0.9s

Figure 10 (c): Simulated structure of Manganese displaying transient thermal stress distribution in time steps of 0, 0.3, 0.5, 0.7 and 0.9s

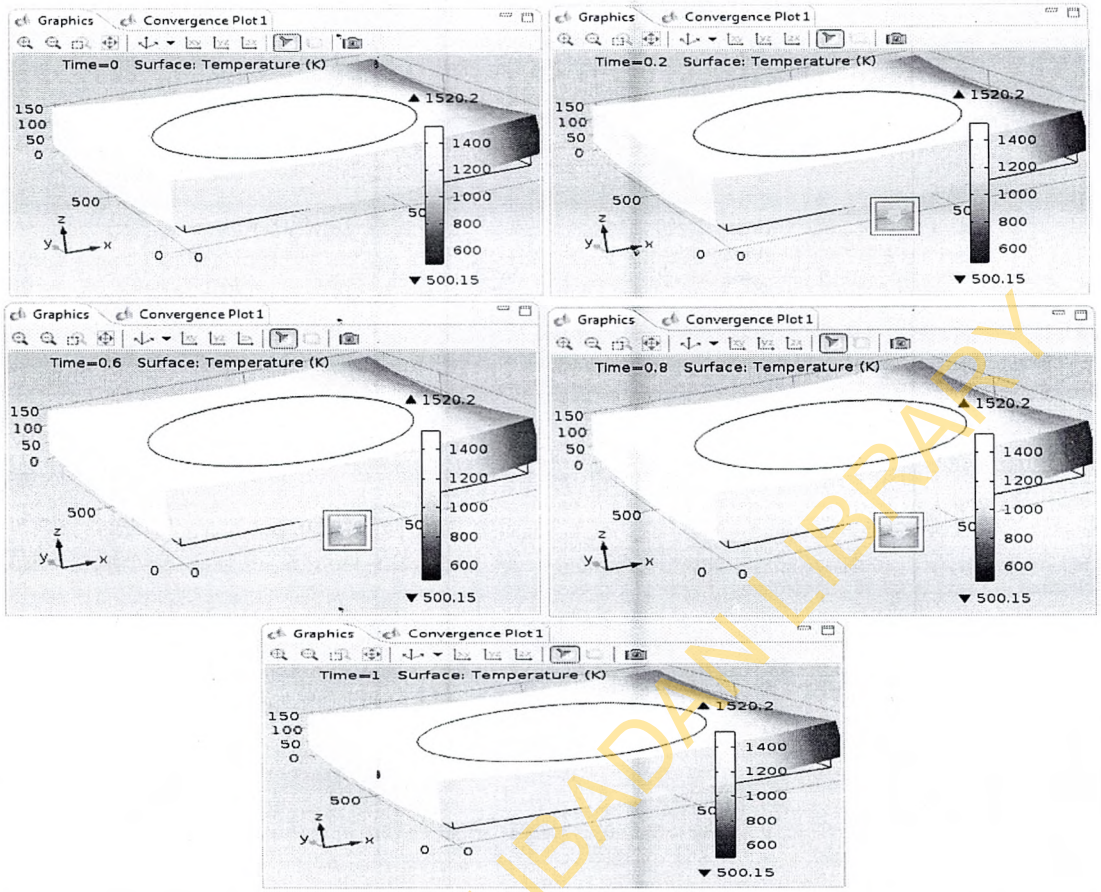

Figure 10 (d): Simulated structure of Manganese displaying transient temperature distribution in time steps of 0, 0.2, 0.6, 0.8 and 1.0s

Since impinging electron beam conveys thermal energy; this energy results to deformation in the microstructure of the Vanadium and Manganese materials; this deformation is called 'Buckling'.

Vanadium and Manganese structures in Figures 10 (a) to (d) are imparted with a 600nm spot size of electron beam; the Vanadium structure of 1200nm by 1200nm dimension is 265nm thick and the Manganese structure of 1000nm by 1000nm dimension is 110nm thick.

Conclusion

Compound systems like the Kirk-Patrick and Baez, small apertures and obeying the Abbe sine condition, will ensure that astigmatism, coma and chromatic aberrations are reduced or eliminated—leading to good image quality.To eliminate coma specifically, Abbe Sine Condition is satisfied if magnification values are $-1.5 \leq M \leq 1.5$, at $-70^0 \leq \theta' \leq 75^0$ for $-30^0 \leq \theta \leq 30^0$.

From this work, 5.899KeV MnK$\alpha_1$and 4.952KeV VKα_1 soft X-rays with spatial resolution of≥0.45μm will be emitted with emission angles of $\theta_V = 103.2^0$ and$\theta_{Mn} = 86.6^0$ respectively.

The nth zone radius increases with the distance of separation between DPSXRM's electron gun and the zone plate. 5.899KeV MnK$\alpha_1$and 4.952KeV VKα_1 soft X-rays will travel a distance of 2.75mm to form circular patches of radii 2.2mm and 2.95mm respectively. Zone plate with nth zone radius of 1.5mm must be positioned 1.5mm and 2mm from the electron gun if circular patches must be formed from 4.952KeV VKα_1 and 5.899KeV MnK$\alpha_1$soft X-rays respectively.

Regarding how focal length relates to area of patch formed on the FZP, the focal lengths of $0.25\mu m \leq F \leq 1.50\mu m$ and $0.04\mu m \leq F \leq 0.2\mu m$ covered by 4.952KeV VKα_1 and 5.899KeV Mn Kα_1 soft X-rays, will occupy circular patch of area $0.03mm^2 \leq A \leq 0.2mm^2$ respectively.

Results reveal that spatial resolution of $244nm \leq \varsigma \leq 1460nm$ is attainable forfocal lengths of$38.1nm \leq F \leq 229nm$ and $32.0nm \leq F \leq$

1460192*nm* covered by 5.899KeV Mn Kα_1 and 4.952KeV VKα_1 soft X-rays, respectively.

Results from simulation reveal that, since impinging electron beam conveys thermal energy; this energy results to deformation in the microstructure of the Vanadium and Manganese materials; this deformation is called 'Buckling'.

With the aid of the penetrometer, the device is able to engage in, in-situ and ex-situ measurements; it should probe into the subsurface at the rate of 10m in 5minutes 40 seconds—at the rate of 0.5m in 17s.

Generally, this device should be able to image microstructures in earth samples, providing vital details on soil texture, structure, moisture, porosity, strength, with assess to subsurface stratigraphy; additionally the DPSXRM should be able to characterize weathered Quaternary and Tertiary age strata. Based on the robust conclusions drawn, this proposed design (the first phase) of an DPSXRM is fit for high spatial resolution measurement of submicrometer accuracy (of earth samples) fully disambiguating existent enigmas.

References

Adetoyinbo A.A., Bello A.K., Hammed O.S., (2013) Assessment of groundwater pollution in Itagunmodi, South West, Nigeria. Canadian Journal on Scientific and Industrial ResearchVolume 3 Pp 64- 67

Barrett R., (2011), Kirk Patrick-Baez mirrors, European Synchrotron Radiation Facility (ESRF)

Blair J.E. and S.B. Hedges (2004) Molecular Clocks Do Not Support the Cambrian Explosion *Oxford Journals,* Volume 22, issue 3, Pp. 387-390

Bunker, G., (2001), Introduction to XAFS. A Practical Guide to X-ray Absorption Fine Structure Spectroscopy, Cambridge, Cambridge University Press, (2010), P 268Volume 52, Issue 6.

Chao *et al*, (2011) Abundance-Based Similarity Indices and Their Estimation When There Are Unseen Species in Samples *Biometrics Vol.* 62, Pp361–371

Dikedi P.N., X-ray interactions with Potassium Carbide (2011) International Journal of the Physical Sciences Vol. 6(8), pp. 2095-2099, Academic Journals

Dupraz *et al* (2009) Processes of carbonate precipitation in modern microbial mats*Earth-Science Reviews*, Volume 96, Pp 141-162

Eizirik E., Murphy W.J. and S. J. O'Brien (2001) Molecular Dating and Biogeography of the Early Placental Mammal Radiation; *the Journal of Heredity* Volume 2 Pp.212-219

Erwin *et al* (2011), The Cambrian Conundrum: Early Divergence and Later Ecological Success in the Early History of Animals *Science* Volume 334 no. 6059 Pp. 1091-1097

Folkard M. (2005), *A Variable Energy Soft X-ray Microprobe to Investigate Mechanisms of the Radiation- Induced Bystander Effect* Work shop

Pfauntsch S.,(2001), *Developments in Soft X-ray Laboratory Systems for Microscopy and Cellular Probing* in PhD thesis, 159

German Research Centre for Geosciences,(2013),

Haschke M., (2014), Laboratory Micro X-Ray Fluorescence Spectroscopy, *Instrumentation and Applications Springer International Publishing*, Switzerland P 29,

Holtz R. D., Kovacs W. D. (2010), An introduction to Geotechnical engineering, page 13, Prentice-Hall Civil Engineering and Engineering Mechanics Series 2nd edition.

Jones III *et al* (2009) Age, provenance, and tectonic setting of Paleoproterozoic quartzite successions in the southwestern United States *Geological Society of America*,volume 121, Pp. 247-264,

Kees G., (2005), Hand-Held Electronic, Cone Penetrometers for Measuring Soil Strength.

Laan *et al*., (2003), Outline proposal: polarized soft X-ray beamline for magnetism at Diamond, P 1

Liangyuan *et al*, (1983), X-Ray Fluorescence (XRF) Determination of Trace Rare-Earth Elements in Geological Samples Using Ion-Exchange-Resin Membrane Technique, Vol. 2, Issue 2, Chinese Journal of Geochemistry, pp 153-169

Lavery *et al*, (2006) Probe-to-Bone Test for Diagnosing Diabetic Foot Osteomyelitis. American Diabetes Association, diabetes care Department of Surgery, Scott and White Hospital, 703 Highland Spring Lane, Georgetown, TX 78628

Macmillan Cancer Support, (2015) http://www.macmillan.org.uk/Cancerinformation/Cancertypes/Bone/Typesofbonecancer/Chordoma.aspx

Michette A. G. (2007), in *Multi-layer mirror* (Mres lectures on slides).

Michette A. G. (2007)*X-ray Optics; the Optics Encyclopaedia. Wiley-VCH Verlag GmbH and Co. KGaA*

Michette, A. G., (2011), Introduction to XAFS. A Practical Guide to X-ray Absorption Fine Structure Spectroscopy, Cambridge, Cambridge University Press, 2010, 268 pp Volume 52, Issue 6, Kings College London

Minh *et al*, (2002), Fabrication of Silicon Microprobes For Optical Near-Field Applications CRC Press, Pp.47-48

Morris S.C. (2000) The Cambrian "explosion": Slow-fuse or megatonnage?Proceedings of *The National Academy of Sciences of the United States of America;* volume 97 Pp. 4426–4429

National Organisation for Rare Disorders, (2014), https://rarediseases.org/rare-diseases/gorham-stout-disease.

Park T. Khim J. and D.K. Choi (2013) Late Middle Cambrian (Cambrian series 3) Trilobite Faunas From The Lowermost Part of The Sesong Formation, Korea and Their Correlation With *North*

China Journal of Paleontology, volume 6, , Pp. 991–1003

Pfauntsch S., (2001), Developments in Soft X-ray Laboratory Systems for Microscopy and Cellular Probing in PhD thesis, 15,159

Sanderson *et al* (2004) Molecular evidence on plant divergence times. *American Journal of Botany volume* 10 Pp. 1656–1665

Sanloup et al, (2013), Structural change in molten basalt at deep mantle conditions;*Nature*.

Shu *et al*, (2002) Head and backbone of the Early Cambrian vertebrate *HaikouichthysNature* Volume 421, Pp. 526-529

Sourty *et al*, (2008), Tomographic imaging ultra-thick specimens with nanometer resolution

Wirth K. and Barth A., 2013)X-Ray Fluorescence (XRF), Geochemical Instrumentation and Analysis "Structure of the Earth". *Fundamentals of Physical Geography, 2nd Edition*. Date Viewed.